2014 IEEE/RSJ International Conference on
Intelligent Robots and Systems (IROS 2014)
September 14-18, 2014, Chicago, IL, USA

Multi-Muscle FES Control of the Human Arm for Interaction Tasks—Stabilizing with Muscle Co-Contraction and Postural Adjustment: A Simulation Study

Yu-Wei Liao, Eric M. Schearer, Eric J. Perreault, Matthew C. Tresch, and Kevin M. Lynch

Abstract— **In this paper we present a method to stimulate multiple muscles in a human arm to perform interaction tasks, using an implanted Functional Electrical Stimulation (FES) neuroprosthesis. The unstable effect arising from interaction tasks is considered, and the arm stability is directly treated as one of the control objectives in the controller design. By exploiting the kinematic and muscular redundancy of the system, we can control the interaction force and the arm's stiffness property simultaneously, thus ensuring the stable execution of interaction tasks. A representative example of such interaction tasks, namely the "pushing with a stick" task, is simulated. It is found that using our proposed controller, as compared to a previously developed feedforward FES controller that does not consider arm stiffness or stability, the stability of the arm is guaranteed while the task of force control is correctly achieved.**

I. Introduction

Functional electrical stimulation (FES) is a promising technology for activating muscles and restoring lost functions to patients with spinal cord injuries. The long-term goal of this study is to develop an FES-control strategy to restore the ability to perform interaction tasks to people with paralyzed arms. Many FES controllers have been developed previously aiming at restoring the lost functions to people with paralyzed limbs, as were surveyed by Lynch and Popovic [1], and Zhang et al. [2]. While these controllers focus on the capability of the muscles that can be stimulated to restore the lost functions, they have not taken into consideration the unstable nature of interaction tasks.

Many interaction tasks in our daily lives are inherently unstable. For example, tightening a screw with a screwdriver or pushing through a stick compromises the stability in directions perpendicular to the tool [3][4]. To successfully execute these unstable tasks, the mechanical stability of the coupled arm–hand-tool system needs to be achieved. In robotics community, such stability is generally achieved using feedback control, but there are many challenges associated with implementing an FES feedback controller. These include the low stimulation rates typical for FES systems and the delays that can lead to feedback instabilities [5]. In control theory it is well known that stabilizing an unstable system generally requires high-frequency feedback, which is yet to be feasible using FES.

An alternative strategy that is commonly utilized by unimpaired humans is feedforward regulation of the stiffness of the arm [6], either by muscle co-contraction [7] or by adjusting the arm posture [8]. Recently strategies for feedforward control of the stiffness of an arm has been introduced to the robotics community and gives rise to the design and control of variable stiffness actuators [9]. These robots, typically equipped with muscle-like actuators and redundant kinematic degrees-of-freedom (DoFs), exploit the redundancy to achieve a certain stiffness profile which helps accomplishing desired behaviors, such as throwing [10] and kicking [11]. However, to our knowledge, similar attempts have not yet been implemented to the FES controllers beyond the purpose of tremor suppression through muscle co-contraction [12], mainly due to the inability to predict the multi-joint stiffness of the arm under FES control. Recently it has been shown that the stiffness of an intact limb can be predicted by a musculoskeletal model incorporating the short-range stiffness (SRS) property of muscles [13][14]. Based on these studies, more recently we have developed a computational model to predict the stiffness and characterize the stability of the arm under FES control for postures throughout the workspace [15].

The purpose of this study is to build on the computational model to develop an FES controller that can exploit both muscular and kinematic redundancy to regulate the stiffness of the arm, in order to achieve arm stability while accomplishing the task of generating interaction force. The proposed controller is currently formulated as an optimization, and can be used as a real-time controller if evaluated quickly enough. To demonstrate the effectiveness of our proposed controller, a representative interaction task, namely the "pushing with a stick" task has been simulated. Both the proposed controller and a previously developed feedforward FES force controller that does not consider stability [16] are tested on the simulated task, and the performance using the two controllers is evaluated. Based on the results, our proposed controller has shown to be effective in achieving both objectives of force control and arm stability, while the previously developed controller is only able to achieve the objective of force control.

This work is supported by NSF grant 0932263.

Y-W Liao and E. M. Schearer, Dept. of Mechanical Engineering, Northwestern University, Evanston, IL {ywl@u.northwestern.edu, eschearer@u.northwestern.edu}

E. J. Perreault and M. C. Tresch, Dept. of Biomedical Engineering and Dept. of Physical Medicine and Rehabilitation, Northwestern University, Evanston, IL {e-perreault@northwestern.edu, m-tresch@northwestern.edu}

K. M. Lynch, Dept. of Mechanical Engineering and the Northwestern Institute on Complex Systems, Northwestern University, Evanston, IL {kmlynch@nortwestern.edu}

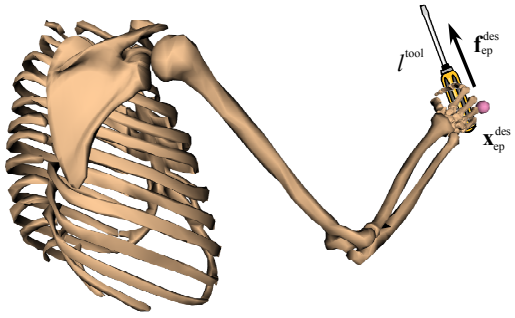

Fig. 1. Schematic drawing of a human (skeleton) generating interaction force through a hand-tool.

The paper is organized as follows. Section II presents the description of the class of problems that are considered. Section III presents the models that are used in this study, as well as provides the derivations of the two objectives: force control and arm stability control. Section IV presents the mathematical formulation of the problem that is considered, and the dimension reduction approach that is used to simplify the problem. Section V presents the simulated task of "pushing with a stick," with the results of using both the baseline and proposed controller. Finally Section VI summarizes the study and addresses discussions.

II. Problem Statement

Given

- a desired Cartesian location of the endpoint of the arm $\mathbf{x}_{\text{ep}}^{\text{des}} \in \mathbb{R}^{3\times 1}$,
- a stick-like hand-tool of length l^{tool} to be held, assuming a ball-and-socket attachment between the endpoint of the arm and the hand-tool, and
- a desired endpoint force $\mathbf{f}_{\text{ep}}^{\text{des}} \in \mathbb{R}^{3\times 1}$ to be applied along the axis of the hand-tool,

we want to find the arm posture $\mathbf{q} \in \mathbb{R}^{n\times 1}$ for its n kinematic degrees-of-freedom (DoFs) and the activations $\boldsymbol{\alpha} \in \mathbb{R}^{m\times 1}$ for its m muscles that can be stimulated, to produce $\mathbf{f}_{\text{ep}}^{\text{des}}$ at the endpoint location $\mathbf{x}_{\text{ep}}^{\text{des}}$ through the hand-tool, while ensuring the stability of the arm during the execution of the task. Fig. 1 gives an illustration of this class of interaction tasks. In multiple-muscle FES neuroprosthesis, there are generally more muscles that can be stimulated than the kinematic DoFs of the arm (i.e. $m > n$), and the arm has more kinematic DoFs than the Cartesian specification of the endpoint location (i.e. $n > 3$), therefore the system has both muscular and kinematic redundancy with respect to the task.

III. Model of a Human Arm Driven by FES Neuroprosthesis

A. 3-D musculoskeletal model of a human arm

The musculoskeletal model of the upper extremity developed by Holzbaur et al. [17] is implemented in the OpenSim environment [18] in this study. The model incorporates kinematic representations for the shoulder and elbow joints, and includes 37 muscle segments. Our simulations consider five kinematic degrees-of-freedom (DoFs): three at the shoulder and two at the elbow, while the wrist joint is considered fixed. Among the 37 muscle segments, 16 segments are chosen to represent the muscles that can be activated by an implanted FES neuroprosthesis [19] (Subject 1). They are: biceps (BIClong and BICshort), brachialis (BRA), deltoid (DELT1, DELT2, and DELT3), infraspinatus (INFSP), latissimus dorsi (LAT1, LAT2, and LAT3), upper pectoralis (PECM1), lower pectoralis (PECM3), pronator teres (PT), supraspinatus (SUPSP), and lateral and medial heads of triceps (TRIlat and TRImed). In addition, we scale the maximum isometric force of the FES-activated muscles to 50% of their nominal values that appear in the original arm model, to capture the reduced force-generating capability of muscles artificially activated using FES [20]. The inertial parameters are taken from Winter [21].

B. Force control

The equation of motion of the arm, using FES-activated muscles as actuators, can be written as

$$M(\mathbf{q})\ddot{\mathbf{q}} + \mathbf{c}(\mathbf{q},\dot{\mathbf{q}}) + \mathbf{g}(\mathbf{q}) = \boldsymbol{\tau}^{\text{m}} + J(\mathbf{q})^{\text{T}}\mathbf{f}_{\text{ep}}^{\text{ext}}, \tag{1}$$

where $\mathbf{q} \in \mathbb{R}^{5\times 1}$ is the vector of joint angles that uniquely defines an arm posture, M, $\mathbf{c}$, and $\mathbf{g}$ are the inertial, centrifugal and Coriolis, and gravitational terms respectively, $\boldsymbol{\tau}^{\text{m}} \in \mathbb{R}^{5\times 1}$ is the torque produced by FES-actuated muscles, $\mathbf{f}_{\text{ep}}^{\text{ext}} \in \mathbb{R}^{3\times 1}$ is the external force applied at the endpoint, and $J(\mathbf{q}) \in \mathbb{R}^{3\times 5}$ is the Jacobian that transforms the external force to joint torque.

In endpoint force control tasks, like the problem defined above, the arm is at equilibrium, and the external endpoint force is the reaction force of the desired endpoint force $\left(\mathbf{f}_{\text{ep}}^{\text{ext}} = -\mathbf{f}_{\text{ep}}^{\text{des}}\right)$, thus equation (1) is reduced to

$$\mathbf{g}(\mathbf{q}) = \boldsymbol{\tau}^{\text{m}} - J(\mathbf{q})^{\text{T}}\mathbf{f}_{\text{ep}}^{\text{des}}. \tag{2}$$

The muscle torque $\boldsymbol{\tau}^{\text{m}}$ is the product of muscle moment arms and muscle-fiber forces, which are limited to the posture-dependent maximum achievable muscle forces, $\mathbf{f}_0^{\text{m}}(\mathbf{q})$,

$$\begin{aligned}\boldsymbol{\tau}^{\text{m}} &= R(\mathbf{q})^{\text{T}}\mathbf{f}^{\text{m}}(\boldsymbol{\alpha},\mathbf{q}) \\ &= R(\mathbf{q})^{\text{T}}\left[\boldsymbol{\alpha}\mathbf{f}_0^{\text{m}}(\mathbf{q})\right],\end{aligned} \tag{3}$$

where $\boldsymbol{\alpha} = [\alpha_1, \alpha_2, ..., \alpha_{16}]$ is the vector of muscle activations with $\alpha_i \in [0,1]$, and $R(\mathbf{q}) \in \mathbb{R}^{16\times 5}$ is the matrix of muscle moment arms.

By rearranging and combining equations (2) and (3), we have the objective of **force control** as

$$R(\mathbf{q})^{\text{T}}\left[\boldsymbol{\alpha}\mathbf{f}_0^{\text{m}}(\mathbf{q})\right] = \mathbf{g}(\mathbf{q}) + J(\mathbf{q})^{\text{T}}\mathbf{f}_{\text{ep}}^{\text{des}}. \tag{4}$$

Additional kinematic constraints that we consider here are:

- the endpoint position of the arm needs to be at the desired endpoint position, $L(\mathbf{q}) = \mathbf{x}_{\text{ep}}^{\text{des}}$, where $L(\mathbf{q})$ is the forward kinematics which maps the vector of joint angles $\mathbf{q}$ to the Cartesian location of endpoint, and
- the palmar surface of the hand needs to be vertical.

The first constraint is obvious, as initially stated in the problem statement. The second constraint is inspired by the normal usage of hand-tools, as will be described later.

It is important to point out that the force control objective

(4), while satisfying the constraints above, is redundant, since the total DoFs (the number of muscles that can be stimulated plus the number of kinematic DoFs of the arm) is larger than the number of joint torques and constraints. As will be discussed subsequently, such redundancy can be exploited to fulfill the secondary objective: the stability of the arm.

C. Arm stability control

A key factor that leads to successful execution of interaction tasks is the stability of the arm system. To achieve arm stability, in this work we explore the control of the stiffness property of the arm by exploiting the muscular and kinematic redundancies. Recently it has been shown that the stiffness of a limb can be predicted by a musckuloskeletal model incorporating the short-range stiffness (SRS) property of muscles [13][14], and based on above, more recently we have developed a model which estimates the intrinsic joint stiffness of the arm under FES control [15] as

$$K_{\mathrm{J}}^{\mathrm{int}}(\boldsymbol{\alpha},\mathbf{q}) = R(\mathbf{q})^{\mathrm{T}} K^{\mathrm{SRS}}(\boldsymbol{\alpha},\mathbf{q}) R(\mathbf{q}) + \frac{\partial R(\mathbf{q})}{\partial \mathbf{q}}^{\mathrm{T}} \mathbf{f}^{\mathrm{m}}(\boldsymbol{\alpha},\mathbf{q}) - \frac{\partial \mathbf{g}(\mathbf{q})}{\partial \mathbf{q}}, \tag{5}$$

where the second term corresponds to the equivalent stiffness resulting from the change of muscle moment arms to the change of joint angles, and the third term is the equivalent stiffness reflecting how the gravitational torques change with joint angles. In the first term $K^{\mathrm{SRS}}(\boldsymbol{\alpha},\mathbf{q}) = \mathrm{diag}\left([k_1^{\mathrm{SRS}}, k_2^{\mathrm{SRS}}, ..., k_{16}^{\mathrm{SRS}}]\right)$ where k_i^{SRS} is the SRS of the i-th muscle-tendon unit, and its calculation, detailed in [22], is briefly reviewed here. This calculation assumes the SRS for the entire muscle-tendon unit can be described by the series connection of an elastic tendon with stiffness k_i^{t} in series with a muscle with force-dependent stiffness k_i^{m}. The net stiffness for each muscle-tendon unit is then given by

$$k_i^{\mathrm{SRS}} = \frac{k_i^{\mathrm{m}} k_i^{\mathrm{t}}}{(k_i^{\mathrm{m}} + k_i^{\mathrm{t}})}. \tag{6}$$

The stiffness of the contracting muscle is dependent on the force within that muscle, f_i^{m}, as follows

$$k_i^{\mathrm{m}} = \frac{\gamma f_i^{\mathrm{m}}(\alpha_i,\mathbf{q})}{L_{\mathrm{m}}^0}, \tag{7}$$

where L_{m}^0 is the optimal muscle length, and γ is a dimensionless scaling constant ($\gamma = 23.4$) used for all muscles [22]. The tendon stiffness is defined by the slope of the generic, dimensionless force-strain curve [23], and then scaled for each individual muscle-tendon unit. Passive joint properties are excluded in the model.

In addition to intrinsic joint stiffness $K_{\mathrm{J}}^{\mathrm{int}}$, the task of generating interaction force through a hand-tool can cause external destabilizing stiffness, as follows

$$\begin{aligned} K_{\mathrm{J}}^{\mathrm{ext}}(\mathbf{q}) &= \frac{\partial \boldsymbol{\tau}^{\mathrm{ext}}}{\partial \mathbf{q}} = \frac{\partial}{\partial \mathbf{q}}\left[-J(\mathbf{q})^{\mathrm{T}} \mathbf{f}_{\mathrm{ep}}^{\mathrm{des}}\right] \\ &= -\frac{\partial J(\mathbf{q})}{\partial \mathbf{q}}^{\mathrm{T}} \mathbf{f}_{\mathrm{ep}}^{\mathrm{des}} - J(\mathbf{q})^{\mathrm{T}} \frac{\partial \mathbf{f}_{\mathrm{ep}}^{\mathrm{des}}}{\partial \mathbf{q}} \\ &= -\frac{\partial J(\mathbf{q})}{\partial \mathbf{q}}^{\mathrm{T}} \mathbf{f}_{\mathrm{ep}}^{\mathrm{des}} - J(\mathbf{q})^{\mathrm{T}} \frac{\partial \mathbf{f}_{\mathrm{ep}}^{\mathrm{des}}}{\partial \mathbf{x}} \frac{\partial \mathbf{x}}{\partial \mathbf{q}} \\ &= -\frac{\partial J(\mathbf{q})}{\partial \mathbf{q}}^{\mathrm{T}} \mathbf{f}_{\mathrm{ep}}^{\mathrm{des}} + J(\mathbf{q})^{\mathrm{T}} K_{\mathrm{ep}}^{\mathrm{tool}} J(\mathbf{q}). \end{aligned} \tag{8}$$

The first term stems from the change of the Jacobian of the arm depending on the joint positions, as discussed in [4]. The second term, which will be zero if the endpoint of the arm is to interact with the environment directly, highlights the extra destabilizing effect arising from the usage of hand-tools. Generating interaction force through a hand-tool introduces an extra destabilizing stiffness at directions perpendicular to the axis of hand-tool, as suggested by Rancourt and Hogan [3]. For instance, if the interaction force is in the z-(vertical) direction, the endpoint-level destabilizing stiffness from the hand-tool can be written as

$$K_{\mathrm{ep}}^{\mathrm{tool}} = \mathrm{diag}\left(\left[\frac{|\mathbf{f}_{\mathrm{ep}}^{\mathrm{des}}|}{l^{\mathrm{tool}}}, \frac{|\mathbf{f}_{\mathrm{ep}}^{\mathrm{des}}|}{l^{\mathrm{tool}}}, 0\right]\right). \tag{9}$$

In this study, the combination of intrinsic joint stiffness $K_{\mathrm{J}}^{\mathrm{int}}$ and external destabilizing stiffness $K_{\mathrm{J}}^{\mathrm{ext}}$ provides a sufficient evaluation to the stability of the arm. The eigenvalues of the combined joint stiffness matrix are used to determine the stability of the arm, and therefore the objective of **arm stability control** can be written as:

$$\begin{aligned} &\text{The system, described by} (\boldsymbol{\alpha}^0, \mathbf{q}^0), \text{ is stable if} \\ &\forall\ \mathrm{Re}\left\{\mathrm{eig}\left[K_{\mathrm{J}}^{\mathrm{int}}(\boldsymbol{\alpha}^0,\mathbf{q}^0) + K_{\mathrm{J}}^{\mathrm{ext}}(\mathbf{q}^0)\right]\right\} < 0. \end{aligned} \tag{10}$$

If all eigenvalues of the combined joint stiffness matrix are negative, the static restoring torques in response to any imposed joint displacement will be in directions opposing the displacement. Therefore the arm will restore to its original posture, as the viscous properties during the maintenance of posture are dissipative [24], and the arm is open-loop stable.

IV. Controller design

A. Mathematical formulation of the original problem

With the mathematical formulations as described in the previous section, now we can derive the formulation of the original problem, by combining both of the objectives: force control (4) and arm stability control (10). Because the arm system has more total DoFs (the sum of kinematic DoFs and muscular DoFs) than the task requirements, optimization is used to resolve the redundancy. A cost function minimizing the sum of squared muscle activations is used, as suggested by Anderson [25]:

$$\begin{aligned} C = \underset{\boldsymbol{\alpha},\mathbf{q}}{\text{minimize}} \quad & \|\boldsymbol{\alpha}\|^2 \\ \text{subject to} \quad & 0 \le \alpha_i \le 1 \\ & L(\mathbf{q}) = \mathbf{x}_{\mathrm{ep}}^{\mathrm{des}} \\ & \text{palm constrained vertical} \\ & R(\mathbf{q})^{\mathrm{T}}\left[\boldsymbol{\alpha}\mathbf{f}_0^{\mathrm{m}}(\mathbf{q})\right] = \mathbf{g}(\mathbf{q}) + J(\mathbf{q})^{\mathrm{T}} \mathbf{f}_{\mathrm{ep}}^{\mathrm{des}} \\ & \mathrm{Re}\left\{\mathrm{eig}\left[K_{\mathrm{J}}^{\mathrm{int}}(\boldsymbol{\alpha},\mathbf{q}) + K_{\mathrm{J}}^{\mathrm{ext}}(\mathbf{q})\right]\right\} < 0. \end{aligned} \tag{11}$$

In (11) we only require the eigenvalues of the combined joint stiffness matrix to have negative real components, and no stability margin for error is considered yet. The zero on the right hand side can be modified to a negative number, if a stability margin is desired.

This optimization is high-dimensional and contains local

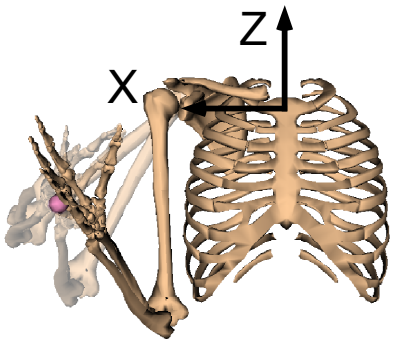

Fig. 2. The 1-D kinematic null space. Muscles are excluded for clarity. The pink ball is the location of the defined endpoint. Three different postures within the null space for this particular endpoint are shown. The orientation of the cooridnate system used in this study is also shown. The origin is coincident with Incisura Jugularis. The x-, y-, and z-axes are in the lateral, anterior, and vertical directions, respectively.

minima. Moreover, the muscular and kinematic parameters have to be evaluated in the Opensim at each iteration of the optimization, which is too slow for real-time implementation. An alternative, as suggested by [26], is to import the full musculoskeletal model into the MATLAB ahead of time, so as to enable real-time evaluation of the muscular parameters. Inspired by this approach, we further developed a dimension reduction method to directly parameterize the kinematic null space and import the muscular parameters only at postures within this relatively small null space, as explained below.

B. Dimension reduction of the kinematics

The endpoint of the arm is defined to be along the axis of pronation/supination at a distance from the elbow corresponding to the location of the knuckles. This corresponds approximately to the 5^{th} metacarpophalangeal joint. The endpoint is described in Cartesian coordinates (x, y, and z), whereas there are five DoFs for the joint space coordinate system. The mismatch in dimensions creates a 2-D null space in which the joint angles can vary arbitrarily while the same endpoint position is achieved. To reduce the dimension of the problem we pose one more constraint on the elbow pronation/supination angle such that the palmar surface of the hand is always vertical. This constraint is chosen because of its functional relevance: it resembles the postures that humans often use in daily tasks, such as holding a fork during eating, or holding a water cup when drinking. Moreover, it has been shown that the elbow pronation/supination angle does not have a substantial effect on the joint stiffness [8]. With this additional constraint, now we are left with a 1-D null space that can be parameterized by the angle of shoulder elevation q_2. For a specified endpoint location, we discretize the 1-D null space in $q_2 \in [0°, 90°]$, evaluate and report the muscular parameters from OpenSim to MATLAB, the environment where all subsequent computations take place. Fig. 2 shows an example of the 1-D kinematic null space for a specified Cartesian location of the endpoint. Muscular parameters at these discrete arm postures are then interpolated using cubic spline fit function in MATLAB for the use in the optimization routine.

C. Simplified problem formulation

We use the aforementioned four kinematic constraints, three for the endpoint location and one for the palm surface vertical, and parameterize the remaining 1 DoF by q_2. Therefore, we arrive at a simplified formulation of the problem:

$$\begin{aligned} C = \underset{\boldsymbol{\alpha}, q_2}{\text{minimize}} \quad & \|\boldsymbol{\alpha}\|^2 \\ \text{subject to} \quad & 0 \le \alpha_i \le 1 \\ & R(q_2)^{\mathrm{T}} \left[\boldsymbol{\alpha}\mathbf{f}_0^{\mathrm{m}}(q_2)\right] = \mathbf{g}(q_2) + J(q_2)^{\mathrm{T}}\mathbf{f}_{\mathrm{ep}}^{\mathrm{des}} \\ & \mathrm{Re}\left\{\mathrm{eig}\left[K_{\mathrm{J}}^{\mathrm{int}}(\boldsymbol{\alpha}, q_2) + K_{\mathrm{J}}^{\mathrm{ext}}(q_2)\right]\right\} < 0. \end{aligned} \tag{12}$$

The MATLAB function fmincon() is used to solve this simplified optimization problem.

V. Simulated Experiments

A. "Pushing with a stick" task

The goal of this study is to develop a controller to restore the ability for paralyzed subjects to perform functional interaction tasks in daily life. For this purpose we simulate the task of "pushing with a stick" as a representative of these interaction tasks. The task requirement is described below:

- The desired endpoint location of the arm is set to be in front of the sternum at a distance of about half length of the arm, $\mathbf{x}_{\mathrm{ep}}^{\mathrm{des}} = [0.00, 0.27, -0.05](\mathrm{m})$. The orientation of the coordinate system used is shown in Fig. 2.
- The length of the hand-tool is set to be 0.1m, $l^{\mathrm{tool}} = 0.1(\mathrm{m})$, and is held in the z-(vertical) direction,
- The desired endpoint force is along the axis of the hand-tool, in the z-(vertical) direction, $\mathbf{f}_{\mathrm{ep}}^{\mathrm{des}} = [0, 0, 30](\mathrm{N})$.

The presented controller is tested on the simulated task. The initial condition is set as: $q_{2_0} = 50°$, and $\alpha_{i_0} = 0.01\%$ for every muscle. A previously developed feedforward FES force controller that does not take into account the arm stability [16] is used as a baseline controller. Since the baseline controller does not select an arm posture on its own, we choose the posture $\mathbf{q}_g$ that results in minimal amount of gravitational potential energy along the null space of $\mathbf{x}_{\mathrm{ep}}^{\mathrm{des}}$, as was done previously [15], and the vector of muscles activations is then computed as follows

$$\begin{aligned} C = \underset{\boldsymbol{\alpha}}{\text{minimize}} \quad & \|\boldsymbol{\alpha}\|^2 \\ \text{subject to} \quad & 0 \le \alpha_i \le 1 \\ & R(\mathbf{q}_g)^{\mathrm{T}} \left[\boldsymbol{\alpha}\mathbf{f}_0^{\mathrm{m}}(\mathbf{q}_g)\right] = \mathbf{g}(\mathbf{q}_g) + J(\mathbf{q}_g)^{\mathrm{T}}\mathbf{f}_{\mathrm{ep}}^{\mathrm{des}}. \end{aligned} \tag{13}$$

B. Analysis of the simulated task

The objective of achieving the desired force is encoded as a hard constraint in both the baseline and proposed controller. Therefore, if either controller is able to find solutions to its individual optimization problem, it means the force control objective is achieved correctly in computer simulation.

To demonstrate the ability of our proposed controller to stabilize the arm posture while achieving the desired force, we compute the eigenvalues of the summed joint stiffness matrix, $K_{\mathrm{J}}^{\mathrm{sum}} = K_{\mathrm{J}}^{\mathrm{int}} + K_{\mathrm{J}}^{\mathrm{ext}}$, for both controllers

$$K_{\mathrm{J}}^{\mathrm{sum}} = \mathbf{V}\boldsymbol{\Lambda}\mathbf{V}^{-1}, \tag{14}$$

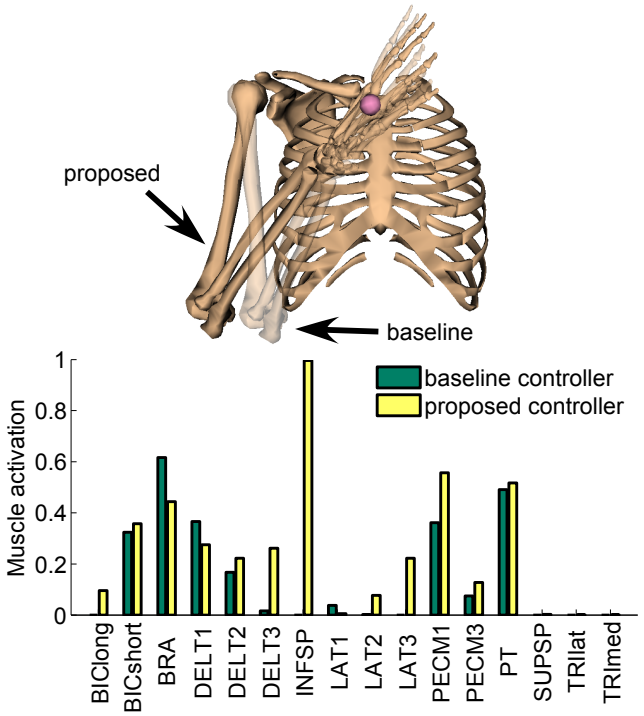

Fig. 3. Comparison between the solutions found using the baseline and proposed controller. (*Top*) the arm posture. The solid arm is the optimal arm posture selected by the proposed controller ($q_2 = 24°$). The faded arm is the posture with minimal gravitational potential energy used by the baseline controller ($q_2 = 16°$). (*Bottom*) the pattern of muscle activations for the 16 muscle segments that can be stimulated by the FES neuroprosthesis.

where $\mathbf{V} = [\mathbf{v}_1, \mathbf{v}_2, ..., \mathbf{v}_5]$ whose i-th column $\mathbf{v}_i \in \mathbb{R}^{5\times 1}$ is the i-th eigenvector of $K_{\mathrm{J}}^{\mathrm{sum}}$, and $\mathbf{\Lambda} = \mathrm{diag}\left([\lambda_1, \lambda_2, ..., \lambda_5]\right)$ with λ_i the eigenvalue of $K_{\mathrm{J}}^{\mathrm{sum}}$ corresponding to $\mathbf{v}_i$.

Moreover, the intrinsic (5) and external stiffness (8) of both controllers are projected to the directions of the eigenvectors of the summed joint stiffness matrix, in order to assess their contributions towards the stability of the arm

$$\begin{aligned} P_i^{\mathrm{int}} &= \mathrm{Proj}_i\left(K_{\mathrm{J}}^{\mathrm{int}}\right) = \mathbf{v}_i^{\mathrm{T}} K_{\mathrm{J}}^{\mathrm{int}} \mathbf{v}_i \\ P_i^{\mathrm{ext}} &= \mathrm{Proj}_i\left(K_{\mathrm{J}}^{\mathrm{ext}}\right) = \mathbf{v}_i^{\mathrm{T}} K_{\mathrm{J}}^{\mathrm{ext}} \mathbf{v}_i \end{aligned} \tag{15}$$

where $\lambda_i = P_i^{\mathrm{int}} + P_i^{\mathrm{ext}}$.

C. Simulation results

Both the baseline and the proposed controller are able to find solutions to their individual optimization problem, however, different arm postures and patterns of muscle activations are used. The optimal arm posture is found to be $q_2 = 24°$ by the proposed controller, whose elbow is slightly more elevated than the posture with minimal gravitational potential energy that is used in the baseline controller ($q_2 = 16°$), as can be seen in Fig. 3(*top*). The patterns of muscle activations are shown in Fig. 3(*bottom*), and it is obvious that the two controllers use recognizably different patterns of muscle activations to achieve the task.

Although at the expense of using higher muscle activations, our proposed controller clearly has the advantage of achieving the stability of the arm. The cost (squared sum of muscle activations) associated with our proposed

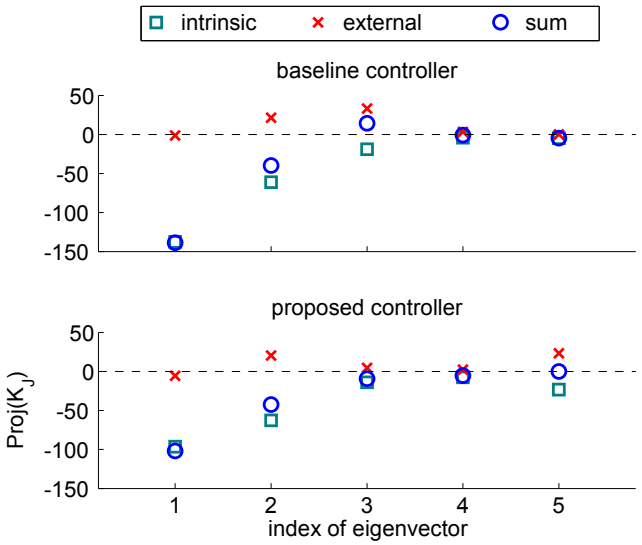

Fig. 4. Comparison of the projections of individual stiffness terms onto the directions of eigenvectors of $K_{\mathrm{J}}^{\mathrm{sum}}$. (*Top*) the result of using the baseline controller. The five eigenvalues of $K_{\mathrm{J}}^{\mathrm{sum}}$ are $[-138.70, -39.72, 14.28, -0.71, -4.64]$. The third eigenvalue is positive, indicating the instability of the corresponding eigenvector. (*Bottom*) the result of using the proposed controller. The five eigenvalues of $K_{\mathrm{J}}^{\mathrm{sum}}$ are $[-101.95, -42.43, -9.36, -5.44, -0.055]$. All five eigenvalues are negative, thus ensures the stability of all DoFs of the arm.

controller is 2.17, which is more than twice as large as the baseline controller (cost = 1.03). However, our proposed controller guarantees all five eigenvalues of the $K_{\mathrm{J}}^{\mathrm{sum}}$ are below zero, which ensures all five DoFs of the arm are stable (Fig. 4(*bottom*)). Contrarily, one of the eigenvalues of the $K_{\mathrm{J}}^{\mathrm{sum}}$ using the baseline controller is greater than zero, indicating the instability along that specific direction of the corresponding eigenvector (Fig. 4(*top*)). If a joint configuration perturbation is applied in this direction of the eigenvector, the response force will be positive and causes further displacement in this direction.

VI. Discussion

The purpose of this study is to develop an FES controller to restore the ability for paralyzed subjects to perform functional interaction tasks. The development is accomplished by incorporating a realistic arm stiffness/stability model to a previously developed feedforward FES force controller, and adding the stability of the arm as a control objective in addition to achieving force control. Based on the results of a simulated interaction task, namely the "pushing with a stick" task, our proposed controller has shown to be effective in ensuring the stability of the arm while achieving the objective of force control. In contrast, the baseline controller fails to stabilize the arm when achieving force control.

While our proposed controller have shown promising results in the simulated tasks, there are a number of limitations that need to be considered. First, to reduce the kinematic dimension to search in, in this study we fix the wrist joint and constrain the palmar surface of the hand to be vertical. These seem to be artificial and rather arbitrary constraints. However, when performing interaction tasks, in particular

those involving the usage of a hand-tool, there are typically specific ways in which the tool works, which will post additional kinematic constraints beyond merely specifying the Cartesian location of the endpoint. These constraints can be used to reduce of the dimension of kinematic redundancy, in ways similar to the method used in this study. Also, there can be additional ways to boost the speed of our proposed controller. In this paper we only reduce the dimensions of kinematic DoFs. However the dimensions of muscular DoFs can potentially be reduced as well. It is possible to find the muscular null space on which all points achieve the objective of force control. Each basis of this muscular null space indicates a specific pattern of muscle co-contractions. The original problem of finding muscle activations can then be reduced to finding the combination of these null space bases that maximizes the stability of the arm, which will be in a lower dimension than the original problem. Moreover, the current controller depends on solving an optimization problem online, which relies heavily on the computation power and does not guarantee to find a feasible solution. Recently, Ajoudani et al. [27] have developed an iterative controller to solve the task of stiffness optimization, with the stability of the controller analyzed. Similar approach may be applied to our optimization problem, and has the potential to achieve a real-time implementable controller for the FES neuroprosthesis. Lastly, in this study we assume a ball-and-socket connection between the endpoint of the arm and the hand-tool. This seems to be a restrictive assumption, as ball-and-socket connections only allow forces in directions aligned with the tool. However, there is a wide range of applications in daily life under this category, such as eating with a fork (we generate downward force while keeping the fork vertical), or tightening using a screwdriver (force applied is aligned with the tool). The effects of tool kinematics as well as its connection to the hand on the stiffness requirement are discussed in detail by Rancourt and Hogan [28]. With our proposed controller which directly takes into account the stiffness and stability, we have the potential to restore the abilities of using various types of tools and accomplishing functional daily tasks using FES neuroprosthesis.

REFERENCES

[1] C. L. Lynch and M. R. Popovic, "Functional electrical stimulation," *IEEE Control Systems Magazine*, Apr 2008.

[2] D. Zhang, T. H. Guan, F. Widjaja, and W. T. Ang, "Functional electrical stimulation in rehabilitation engineering: A survey," in *1st International Convention on Rehabilitation Engineering & Assistive Technology*, 2007.

[3] D. Rancourt and N. Hogan, "Stability in force-production tasks," *Journal of Motor Behavior*, vol. 33, no. 2, 2001.

[4] J. McIntyre, F. A. Mussa-Ivaldi, and E. Bizzi, "The control of stable postures in the multijoint arm," *Exp Brain Res*, vol. 110, 1996.

[5] K. Masani, A. Vette, N. Kawashima, and M. Popovic, "Neuromusculoskeletal torque-generation process has a large destabilizing effect on the control mechanism of quiet standing," *Journal of neurophysiology*, vol. 100, no. 3, 2008.

[6] N. Hogan, "The mechanics of multi-joint posture and movement control," *Biological Cybernetics*, vol. 52, 1985.

[7] P. Gribble, L. Mullin, N. Cothros, and A. Mattar, "Role of cocontraction in arm movement accuracy," *Journal of Neurophysiology*, vol. 89, no. 5, 2003.

[8] R. D. Trumbower, M. A. Krutzy, B.-S. Yang, and E. J. Perreault, "Use of self-selected postures to regulate multi-joint stiffness during unconstrained tasks," *PLoS One*, vol. 4, 2009.

[9] A. Albu-Schaffer, O. Eiberger, M. Grebenstein, S. Haddadin, C. Ott, T. Wimbock, S. Wolf, and G. Hirzinger, "Soft robotics," *Robotics & Automation Magazine, IEEE*, vol. 15, no. 3, 2008.

[10] D. Braun, M. Howard, and S. Vijayakumar, "Optimal variable stiffness control: formulation and application to explosive movement tasks," *Autonomous Robots*, vol. 33, no. 3, 2012.

[11] M. Garabini, A. Passaglia, F. Belo, P. Salaris, and A. Bicchi, "Optimality principles in stiffness control: The vsa kick," in *Robotics and Automation (ICRA), 2012 IEEE International Conference on*, 2012.

[12] A. P. L. Bó and P. Poignet, "Tremor attenuation using fes-based joint stiffness control," in *Robotics and Automation (ICRA), 2010 IEEE International Conference on*. IEEE, 2010.

[13] X. Hu, W. M. Murray, and E. J. Perreault, "Muscle short-range stiffness can be used to estimate the endpoint stiffness of the human arm," *Journal of Neurophysiology*, vol. 105, 2011.

[14] S. Pfeifer, H. Vallery, M. Hardegger, R. Riener, and E. Perreault, "Model-based estimation of knee stiffness," *Biomedical Engineering, IEEE Transactions on*, vol. 59, no. 9, 2012.

[15] Y.-W. Liao, E. M. Schearer, X. Hu, E. J. Perreault, M. C. Tresch, and K. M. Lynch, "Modeling open-loop stability of a human arm driven by a functional electrical stimulation neuroprosthesis," in *35th Annual International Conference of the IEEE Engineering in Medicine and Biology Society (EMBC)*, 2013.

[16] E. M. Schearer, Y.-W. Liao, E. J. Perreault, M. C. Tresch, W. D. Memberg, R. F. Kirsch, and K. M. Lynch, "Multi-muscle fes force control of the human arm for arbitrary goals," *IEEE Transactions on Neural Systems and Rehabilitation Engineering*, 2013.

[17] K. R. Holzbaur, W. M. Murray, and S. L. Delp, "A model of the upper extremity for simulating musculoskeletal surgery and analyzing neuromuscular control," *Annals of Biomedical Engineering*, vol. 33, 2005.

[18] S. L. Delp, F. C. Anderson, A. S. Arnoal, P. Loan, A. Habib, C. T. John, E. Guendelman, and D. G. Thelen, "Opensim: Open-source software to create and analyze dynamic simulations of movement," *IEEE Transactions on Biomedical Engineering*, 2007.

[19] K. H. Polasek, H. A. Hoyen, M. W. Keith, R. F. Kirsch, and D. J. Tyler, "Stimulation stability and selectivity of chronically implanted multicontact nerve cuff electrods in the human upper extremity," *IEEE Transactions on Neural Systems and Rehabilitation Engineering*, vol. 17, no. 5, 2009.

[20] J. G. Hincapie, D. Blana, E. K. Chadwick, and R. F. Kirsch, "Musculoskeletal model-guided, customizable selection of shoulder and elbow muscles for a c5 sci neuroprosthesis," *IEEE Transactions on Neural Systems and Rehabilitation Engineering*, vol. 16, 2008.

[21] D. A. Winter, *Biomechanics and motor control of human movement*. John Wiley & Sons, 2009.

[22] L. Cui, E. J. Perreault, H. Maas, and T. G. Sandercock, "Modeling short-range stiffness of feline lower hindlimb muscles," *Journal of Biomechanics*, vol. 41, 2008.

[23] F. E. Zajac, "Muscle and tendon: properties, models, scaling, and application to biomechanics and motor control," *Critical Review in Biomedical Engineering*, vol. 17, 1989.

[24] E. J. Perreault, R. F. Kirsch, and P. E. Crago, "Multijoint dynamics and postural stability of the human arm," *Experimental brain research*, vol. 157, no. 4, 2004.

[25] F. Anderson and M. Pandy, "Dynamic optimization of human walking," *Journal of biomechanical engineering*, vol. 123, 2001.

[26] E. K. Chadwick, D. Blana, A. J. van den Bogert, and R. F. Kirsch, "A real-time, 3-d musculoskeletal model for dynamic simulation of arm movements," *Biomedical Engineering, IEEE Transactions on*, vol. 56, no. 4, 2009.

[27] A. Ajoudani, M. Gabiccini, N. Tsagarakis, A. Albu-Schäffer, and A. Bicchi, "Teleimpedance: Exploring the role of common-mode and configuration-dependant stiffness," in *IEEE International Conference on Humanoid Robots*, 2012.

[28] D. Rancourt and N. Hogan, "The biomechanics of force production," in *Progress in Motor Control*. Springer, 2009.